Repeated temperature modulation epitaxy for p-type doping and light-emitting diode based on ZnO

ATSUSHI TSUKAZAKI[1], AKIRA OHTOMO[1], TAKEYOSHI ONUMA[2], MAKOTO OHTANI[1], TAKAYUKI MAKINO[3], MASATOMO SUMIYA[4], KEITA OHTANI[5], SHIGEFUSA F. CHICHIBU[2,3], SYUNROU FUKE[4], YUSABUROU SEGAWA[3], HIDEO OHNO[5], HIDEOMI KOINUMA[6,7] AND MASASHI KAWASAKI[1,7]*

[1]Institute for Materials Research, Tohoku University, Sendai 980-8577, Japan
[2]Institute of Applied Physics and Graduate School of Pure and Applied Sciences, University of Tsukuba, Tsukuba 305-8573, Japan
[3]Photodynamics Research Center, The Institute of Physical and Chemical Research (RIKEN), Sendai 980-0845, Japan
[4]Department of Electrical and Electronic Engineering, Shizuoka University, Hamamatsu 432-8561, Japan
[5]Research Institute of Electrical Communication, Tohoku University, Sendai 980-8577, Japan
[6]Materials and Structures Laboratory, Tokyo Institute of Technology, Yokohama 226-8503, Japan
[7]Combinatorial Material Science and Technology (COMET), Tsukuba 305-0044, Japan
*e-mail: kawasaki@imr.tohoku.ac.jp

Published online: 19 December 2004; doi:10.1038/nmat1284

Since the successful demonstration of a blue light-emitting diode (LED)[1], potential materials for making short-wavelength LEDs and diode lasers have been attracting increasing interest as the demands for display, illumination and information storage grow[2–4]. Zinc oxide has substantial advantages including large exciton binding energy, as demonstrated by efficient excitonic lasing on optical excitation[5,6]. Several groups have postulated the use of p-type ZnO doped with nitrogen, arsenic or phosphorus[7–10], and even p–n junctions[11–13]. However, the choice of dopant and growth technique remains controversial and the reliability of p-type ZnO is still under debate[14]. If ZnO is ever to produce long-lasting and robust devices, the quality of epitaxial layers has to be improved as has been the protocol in other compound semiconductors[15]. Here we report high-quality undoped films with electron mobility exceeding that in the bulk. We have used a new technique to fabricate p-type ZnO reproducibly. Violet electroluminescence from homostructural p–i–n junctions is demonstrated at room-temperature.

Extending semiconductor devices to new compounds has produced great benefits to human life, as exemplified by modern optoelectronic and high-speed electronic devices for communications attained by GaAs-based III–V compounds[16], and blue LEDs and lasers realized by GaN (ref. 1). Even wider-bandgap compounds such as diamond, $Al_xGa_{1-x}N$, BN (refs 2–4) and ZnO have attracted considerable interest for applications in ultraviolet LEDs and lasers and electronic devices durable at high-power and/or high-temperature operation. Among them, ZnO has the following advantages for LEDs and lasers. First, the exciton binding energy in ZnO is as large as 60 meV and can be increased to over 100 meV in superlattices[17]. This exciton stability provides opportunities for making highly efficient lasers operable at room-temperature[5,6]. Second, it is possible to tune the bandgap from 3 eV to 4.5 eV in $Mg_xZn_{1-x}O$ and $Zn_{1-x}Cd_xO$ alloy films with quite small lattice mismatch between the two different compositions[18–20]. This advantage makes it possible to realize strain-free and high-quality quantum wells. Third, large and high-quality single-crystal wafers are commercially available.

To harvest these advantages in real devices, a reliable technique for fabricating p-type doping needs to be established. Compared with other II–VI semiconductors and GaN, it has been difficult to dope ZnO to produce a p-type semiconductor because of a strong self-compensation effect arising from the presence of native defects or hydrogen impurities[21,22]. The first p-type ZnO was claimed in films made by vapour-phase transport[7] in NH_3, followed by molecular-beam epitaxy (MBE) using an atomic nitrogen source[9]. These films had a hole concentration of 10^{16}–10^{17} cm^{-3}. There are other claims[8,10] that As or P doping can achieve hole concentrations higher than 1×10^{18} cm^{-3}. In the former case, it can be naturally understood that nitrogen replaces oxygen to generate holes because of similar ionic radius. But the latter cases have raised the following questions[14]. The ionic radii of P and As seem to be too large to occupy the oxygen site within the wurtzite host lattice and thus to serve as acceptors. Also, from a comparison with established properties of p-type GaN (ref. 12), such a high concentration of holes would not be expected in ZnO. None of the studies mentioned addressed significant effort

©2005 Nature Publishing Group

Figure 1 Thin films of ZnO grown in persisting layer-by-layer mode show high-quality optical and electronic properties. a, RHEED intensity oscillation observed during ZnO thin-film growth by laser MBE at a temperature of 950 °C on an atomically smooth ZnO buffer layer formed on a $ScAlMgO_4$ substrate. The oscillation period corresponds to a 0.26-nm-thick charge-neutral molecular layer grown by about 23 laser pulses. The oscillation persisted over film growth to a thickness of 1 μm. The film has the same lattice constants (a = 0.3250 nm, c = 0.5204 nm) as the bulk values by relaxing the very small lattice mismatch of 0.09% with the SCAM substrate in the high-temperature annealed ZnO buffer layer. The full-width at half-maximum of the rocking curve at the (002) reflection is less than 18 arcsec, which is close to the instrumental resolution. The growth direction is identified, through experiments similar to those reported previously[32], to be $[000\bar{1}]$ of the wurtzite structure (oxygen face). **b**, Photoluminescence (PL) spectrum (inset) and temporal decay of the luminescence intensity at the peak energy (indicated by triangle) for an intrinsic ZnO film. The dashed peak represents the temporal evolution of the excitation laser pulse (Ti: sapphire, 242 nm, 30 mW, 80 fs). The lifetime of free exciton emission exceeds 2.5 ns, indicating the high quality of the sample. **c**, Temperature dependence of electron mobility and carrier concentration for an undoped ZnO film (solid circles) and a ZnO bulk single-crystal (open circles, after Look *et al.*[27]). To ensure that the measurements extract the intrinsic properties of the ZnO film, a fairly thick film (1 μm) was grown on a semi-insulating $Mg_{0.15}Zn_{0.85}O$ buffer layer which was annealed to prepare an atomically smooth surface before the ZnO deposition[23].

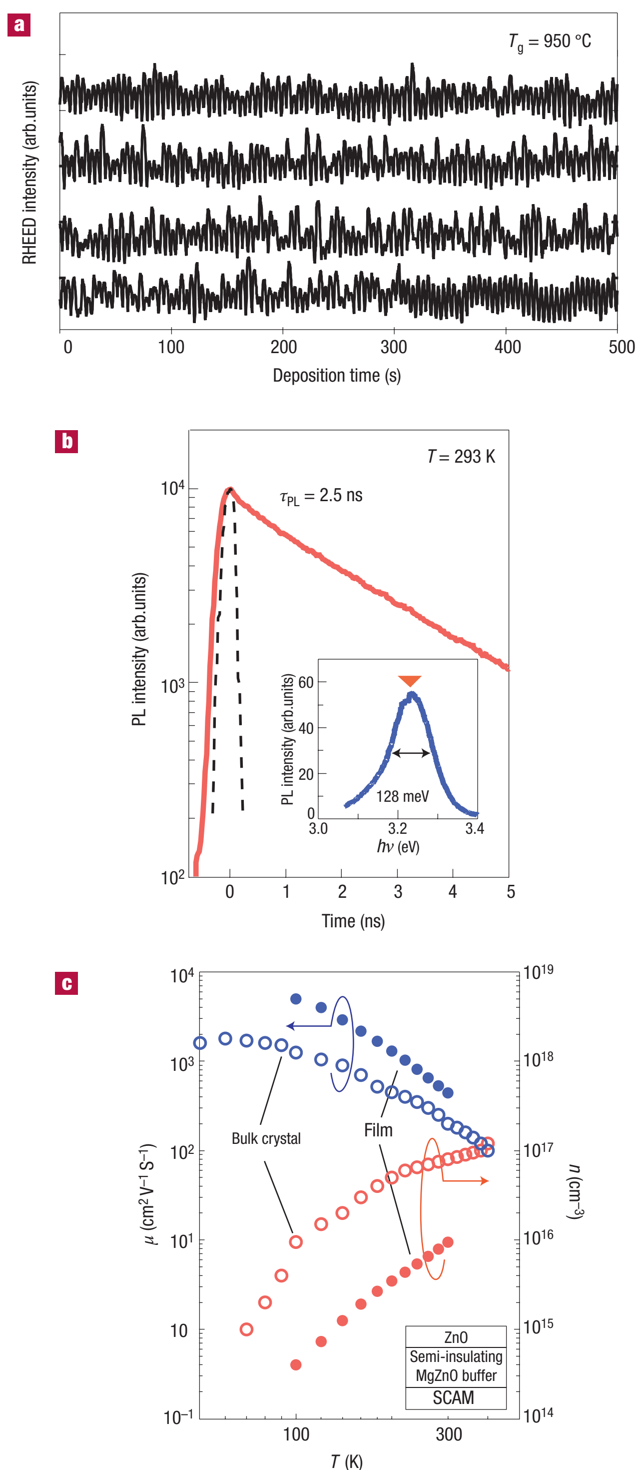

to growing the high-quality undoped films that generally serve as a starting point for reliable doping in semiconductors. Here we propose a repeated temperature modulation (RTM) technique as a reliable and reproducible way to fabricate p-type ZnO.

Thin films of ZnO and junction devices were grown by laser MBE using nitrogen as a p-type dopant (see Methods). Figure 1a shows a typical intensity oscillation of reflection high-energy electron diffraction (RHEED) observed during undoped ZnO film growth at a temperature (T_g) of 950 °C. This layer-by-layer growth mode has become possible with our development of an atomically smooth ZnO buffer layer on $ScAlMgO_4$ (SCAM) substrate produced by high-temperature annealing[23,24]. The undoped ZnO films show excellent optical and electronic properties. Figure 1b shows a photoluminescence spectrum (inset) and temporal variation of the photoluminescence intensity taken at room-temperature. The lifetime (τ_{PL}) of free-exciton emission reaches 2.5 ns. This τ_{PL} is much longer than the value in ZnO crystal (1 ns)[25] or high-quality GaN single crystal (0.86 ns)[26]. Such a long lifetime indicates very low density of non-radiative defects and negligible carrier trapping to deep radiative defects, such as the green luminescence band frequently seen in poor-crystallinity crystals and films. Figure 1c shows the temperature dependence of residual electron density (n) and Hall mobility (μ) for an undoped ZnO film. The value of n is about 1×10^{16} cm^{-3} at room temperature and decreases with decreasing temperature, with an activation energy of about 60 meV. The value of μ is 300 cm^2 V^{-1} s^{-1} and 5,000 cm^2 V^{-1} s^{-1} at 300 K and 100 K, respectively, surpassing the best value for a ZnO bulk single crystal[27]. Therefore, we conclude that ZnO films grown at this high temperature, T_g, on atomically smooth buffer layers can serve as an arena for testing acceptor doping.

However, nitrogen, as one of the most promising acceptor impurities, cannot be incorporated into ZnO at such a high T_g. Nitrogen concentration (C_N) decreases from a few times 10^{20} cm^{-3} at T_g = 450 °C to a few times 10^{18} cm^{-3} at T_g = 700 °C, and at T_g = 950 °C it is lower than the detection limit (mid-10^{17} cm^{-3})[28]. To solve this dilemma, we have developed RTM to satisfy both high crystallinity and high C_N. We repeated a growth sequence in which a nitrogen-doped ZnO (ZnO:N) layer 10–15 nm thick is deposited at low temperature (T_L), followed by rapid ramp to high temperature (T_H), and growth of a 1-nm-thick layer at T_H. Figure 2a shows an example of the time variations of RTM. During the processes, the RHEED pattern switched between two states as shown in the insets of Fig. 2b: streaks (left) at T_L and spots (right) at T_H. The streak length, defined by the full width at half maximum of streak intensity peak in the vertical direction (shown on the insets), is plotted as a function of time in Fig. 2b. During deposition at T_L, the surface became gradually rougher because of the low surface diffusivity of precursors. On rapid ramping to T_H, the surface smoothness recovered quickly. Part of the time variation in Fig. 2b is magnified in Fig. 2c (red)

©2005 Nature Publishing Group

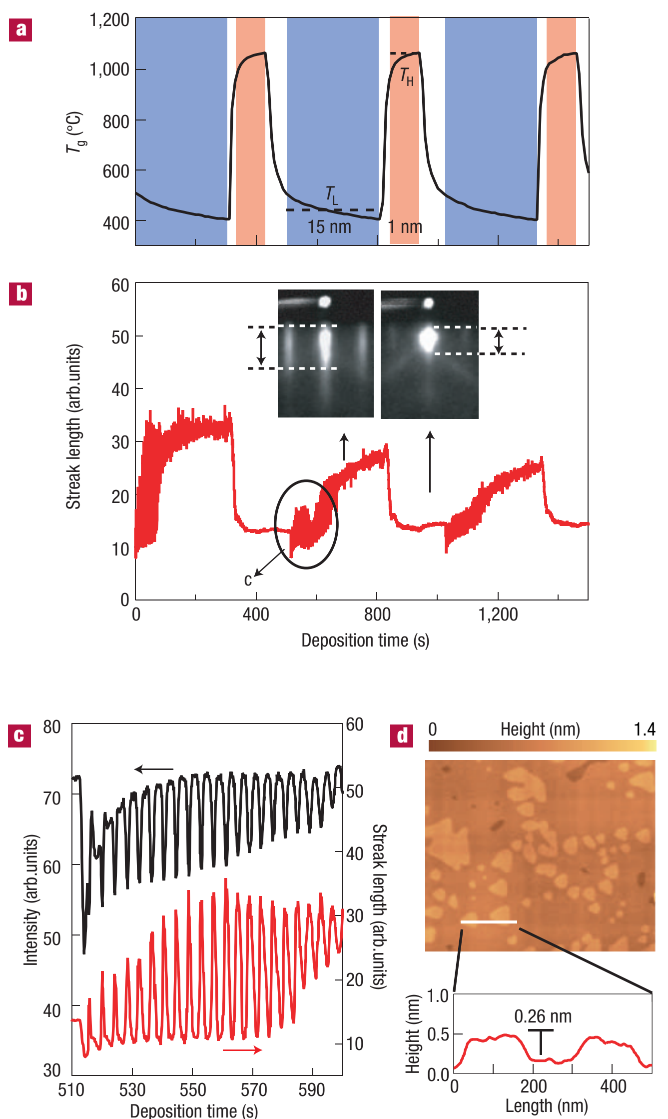

Figure 2 Atomically smooth ZnO films doped with nitrogen can be grown by a repeated temperature modulation technique. a, Temporal variation of growth temperature, switching between T_H and T_L, during ZnO thin-film growth. Layers of ZnO:N with high nitrogen concentration (C_N) were deposited at T_L in the period coloured blue. The layers were annealed and additional ZnO:N layers with low C_N were grown in the period coloured red in order to activate nitrogen as an acceptor and recover surface smoothness, respectively. **b**, Typical RHEED patterns observed during T_L (left) and T_H (right) periods are shown in the insets, representing rather rough and atomically smooth surfaces by streaky and spotty patterns, respectively. Temporal variation of streak length (defined by broken lines) is plotted as a measure of the surface roughness. **c**, RHEED intensity (black) and streak length (red) are plotted for the initial growth of high C_N layer at T_L as denoted by circle in **b**. Clear oscillations having a half-phase shift confirm the layer-by-layer growth mode. **d**, An AFM image of the surface for a 500-nm-thick ZnO:N film. The step height corresponds to the thickness of a charge-neutral molecular layer of ZnO (0.26 nm).

together with the RHEED intensity oscillation (black). The two oscillation patterns have opposite phase, indicating that initial T_L layers grown on atomically flat T_H layers grew in layer-by-layer mode even at such a low temperature. Figure 2d shows an atomic force microscopy image for a ZnO:N film. The surface is composed of

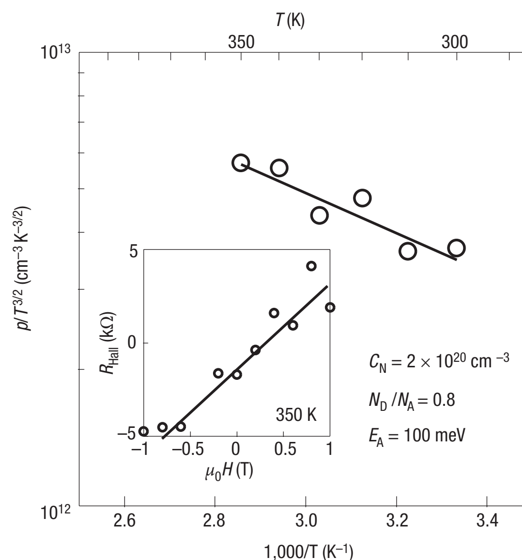

Figure 3 Temperature dependence of hole concentration (p) in a p-type ZnO doped with nitrogen. (Nitrogen concentration $C_N = 2 \times 10^{20}$ cm^{-3}.) A typical variation of the Hall voltage during a magnetic field scan is shown in the inset. The hole mobility varies from 5 cm^2 V^{-1} s^{-1} at 350 K to 8 cm^2 V^{-1} s^{-1} at 300 K. Activation energy E_A and compensation ratio N_D/N_A are deduced to be 100 meV and 0.8, respectively, from the linear fitting[9] of $p = (N_D/N_A - 1)(g_{A1}/g_{A0})N_vT^{3/2}\exp(-E_A/k_BT)$, where $g_{A0} = 4$ and $g_{A1} = 1$ are the unoccupied and occupied state degeneracies, respectively, $N_vT^{3/2} = 2(2\pi m_h k_B T/h^2)^{3/2}$ is the density of states in the valence band, where k_B is Boltzmann's constant and h denotes Planck's constant, and m_h is assumed to be $0.9m_0$ with m_0 being free electron mass.

atomically flat, wide terraces and 0.26-nm-high islands. By using RTM, we can grow ZnO:N films with C_N ranging from several times 10^{20} cm^{-3} to a few times 10^{18} cm^{-3} by tuning T_L from 400 °C to 600 °C. Among these films, those grown at $T_L = 400$ °C and $T_H = 950$ °C reproducibly showed p-type conduction. It is worth mentioning that T_H was chosen to satisfy the condition that hydrogen is completely extracted from the film[29]. Because residual hydrogen in the growth chamber is incorporated in the films during growth[21], high-temperature annealing may be essential not only for annihilating non-equilibrium defects but also for removing hydrogen, if any, to activate the acceptors.

The ZnO:N films prepared by RTM have the same in-plane lattice constant as that of the buffer layer. The out-of-plane lattice constant is slightly expanded (+0.02%) compared with the bulk value. The rocking curve width is as narrow as that of the undoped ZnO films, indicating that the structural quality of the p-type ZnO is very high. The inset of Fig. 3 shows a set of raw data for the Hall resistance, indicating p-type conduction as evidenced by the positive slope. Figure 3 shows hole concentration as a function of temperature for a p-type ZnO:N film with $C_N = 2 \times 10^{20}$ cm^{-3}. From these data, we can deduce an activation energy E_A of 100 meV and compensation ratio $N_D/N_A \approx 0.8$. Here we note that N_D/N_A obtained in the present p-type ZnO film is higher than the reported value of 0.1 for p-type ZnO grown by MBE[9]. Therefore, there is still room to increase hole concentration by tuning the RTM growth condition.

The schematic structure of a typical homostructural p–i–n junction is shown in Fig. 4a, which was grown throughout in layer-by-layer mode keeping an atomically flat interface. Figure 4b shows typical current–voltage characteristics. Fairly good rectification was obtained with a threshold voltage of about 7 V. The threshold

©2005 Nature Publishing Group

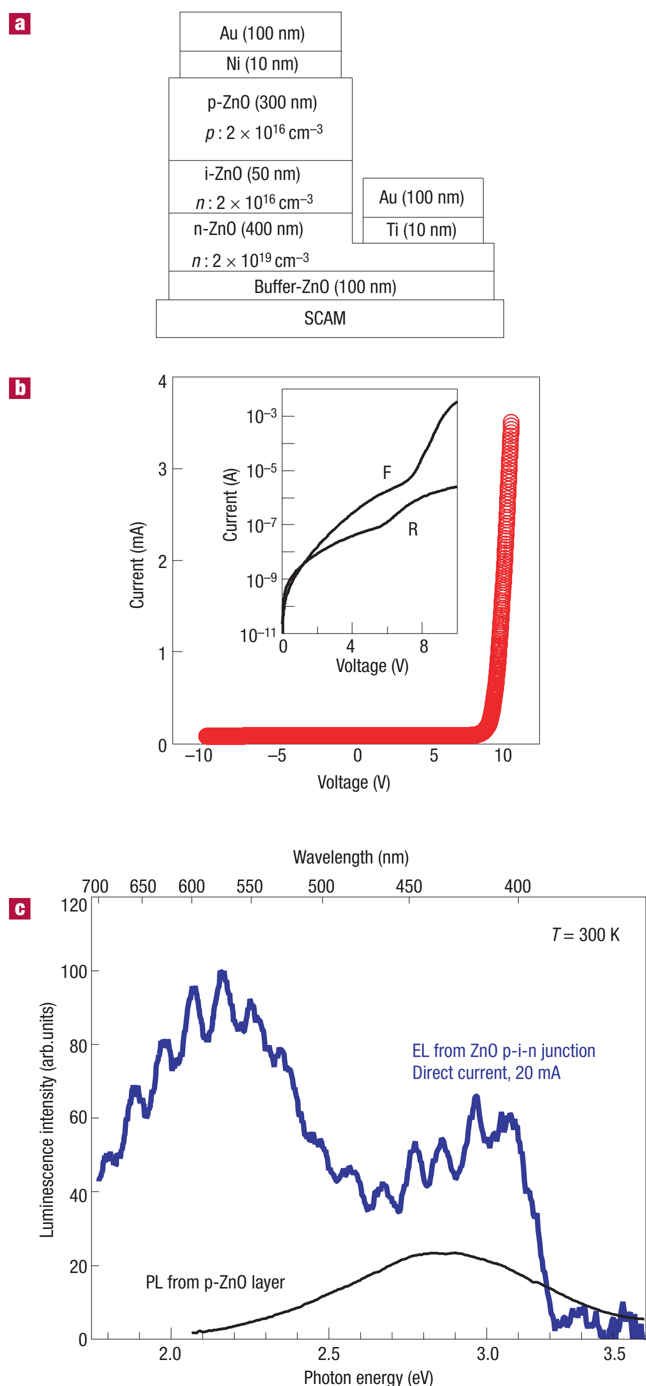

Figure 4 Zinc oxide homostructural p–i–n junction shows rectifying current–voltage characteristics and electroluminescence (EL) in forward bias at room-temperature. a, The structure of a typical p–i–n junction LED. **b**, Current–voltage characteristics of a p–i–n junction. The inset has logarithmic scale in current with F and R denoting forward and reverse bias conditions, respectively. **c**, Electroluminescence spectrum from the p–i–n junction (blue) and photoluminescence (PL) spectrum of a p-type ZnO film measured at 300 K. The p–i–n junction was operated by feeding in a direct current of 20 mA.

voltage is higher than the bandgap of ZnO (3.3 eV), mainly owing to the high resistivity of the p-type ZnO layer. The electroluminescence is measured by feeding in a direct current at room temperature. This spectrum was measured from the top by detecting the light escaping from the edge of the top electrode. The electroluminescence spectrum shows luminescence from violet to green regions with multi-reflection interference fringes. We would expect exciton emission at 3.2 eV from the undoped layer (i-ZnO) as shown in the inset of Fig. 1b, but the electroluminescence spectrum apparently shows a redshift. This is partly due to the low hole concentration in p-type ZnO: electron injection from i-ZnO to p-type ZnO overcomes hole injection from p-type ZnO to i-ZnO. The photoluminescence spectrum (black) of a p-type ZnO film is also shown. The higher-energy side peak around 430 nm in the electroluminescence spectrum matches well with the photoluminescence spectrum. Another factor could be that the electroluminescence from active i-ZnO is partly absorbed in the p-type layer because of a slight redshift of the absorption edge for this layer. Nevertheless, the signal-to-noise ratio of the electroluminescence spectrum shown in Fig. 4c is much better than those reported previously[11,30]. More importantly, the RTM technique established for reliable p-type doping of ZnO enables us to improve the device performance further by optimizing the growth parameters and device structures.

The next challenge will be to increase the hole concentration by further optimizing the growth process of p-type ZnO. Making a p-type (Mg,Zn)O film is also an important challenge, not only to prevent the majority of electrons from injecting into the p-type layers, but also to avoid attenuation of band-edge emission from the i-ZnO.

METHODS

SAMPLE PREPARATION

All films were grown on insulating and lattice-matched $ScAlMgO_4$ (SCAM) substrates by laser MBE equipped with a laser heating system[31]. A semiconductor laser beam was introduced to the back of a substrate susceptor so that very high substrate temperature (~1,000 °C) with clean vacuum and very rapid temperature variation were realized during the growth. These are important factors in this study. Single-crystal ZnO and (Mg,Zn)O ceramic targets were ablated by KrF excimer laser pulses (λ = 248 nm, 5 Hz) with an oxygen flow of 1×10^{-6} torr. The growth direction of the undoped film was determined by means of coaxial impact-collision ion scattering spectroscopy[32]. For nitrogen doping, a radical source was operated at 350 W with a nitrogen flow of 5×10^{-6} torr. During thin-film growth, the RHEED pattern was monitored and the intensity oscillation was recorded for the specularly reflected spot. To grow semiconductor films and avoid such defects as stacking faults, a step-flow growth mode for which RHEED oscillation is absent is usually preferred rather than the layer-by-layer growth mode. However, the almost step-free surface of the ZnO buffer-layer formed on the cleaved SCAM surface makes it difficult to convert the growth mode to step-flow mode, even at such high temperatures. The typical distance between nucleated islands is a few hundred nanometres, as seen in the AFM image shown in Fig. 2d. If step-edges had been provided as in the case of a conventionally polished ZnO substrate surface with a vicinal angle of 0.1° or so, the step-flow mode would have dominated. The films were patterned into Hall bars (220 μm × 60 μm) and the contact metal electrodes were made with Au/Ti for n-type film and Au/Ni for p-type film, giving good ohmic contact. The p–i–n junction devices shown in Fig. 4a were fabricated as follows. On the SCAM substrate, a ZnO buffer layer 100 nm thick was grown at 700 °C and annealed *in situ* at 1000 °C to obtain an atomically smooth surface. Gallium-doped n-type ZnO[31] and i-ZnO layers were grown at 950 °C. A p-type ZnO layer was grown by the process shown in Fig. 2. The junctions with a size of 300 μm × 300 μm were processed as mesa structures by photolithography and argon-ion milling. Ohmic contacts of Au/Ni and Au/Ti were formed on p-type and n-type ZnO, respectively.

Received 28 June 2004; accepted 27 September 2004; published 19 December 2004.

References

1. Nakamura, S., Mukai, T. & Senoh, M. Candela-class high-brightness InGaN/AlGaN double-heterostructure blue-light emitting diodes. *Appl. Phys. Lett.* **64,** 1687–1689 (1994).
2. Kinoshita, A., Hirayama, H., Ainoya, M., Aoyagi, Y. & Hirata, A. Room-temperature operation at 333 nm of $Al_{0.03}Ga_{0.97}N/Al_{0.25}Ga_{0.75}N$ quantum-well light-emitting diodes with Mg-doped superlattice layers. *Appl. Phys. Lett.* **77,** 175–177 (2000).
3. Koizumi, S., Watanabe, K., Hasegawa, M. & Kanda, H. Ultraviolet emission from a diamond pn junction. *Science* **292,** 1899–1901 (2001).
4. Watanabe, K., Taniguchi, T. & Kanda, H. Direct-bandgap properties and evidence for ultraviolet lasing of hexagonal boron nitride single crystal. *Nature Mater.* **3,** 404–409 (2004).
5. Bagnall, D. M. *et al.* Optically pumped lasing of ZnO at room temperature. *Appl. Phys. Lett.* **70,** 2230–2232 (1997).
6. Yu, P. *et al.* Ultraviolet spontaneous and stimulated emissions from ZnO microcrystalline thin films at room temperature. *Solid State Commun.* **103,** 459–463 (1997).
7. Minegishi, K. *et al.* Growth of p-type zinc oxide films by chemical vapor deposition. *Jpn J. Appl. Phys.* **36,** L1453–L1455 (1997).
8. Ryu, Y. R. *et al.* Synthesis of p-type ZnO films. *J. Cryst. Growth* **216,** 330–334 (2000).

©2005 Nature Publishing Group

9. Look, D. C. *et al.* Characterization of homoepitaxial p-type ZnO grown by molecular beam epitaxy. *Appl. Phys. Lett.* **81,** 1830–1832 (2002).
10. Kim, K.-K., Kim, H.-S., Hwang, D.-K., Lim, J.-H. & Park, S.-J. Realization of p-type ZnO thin films via phosphorus doping and thermal activation of the dopant. *Appl. Phys. Lett.* **83,** 63–65 (2003).
11. Aoki, T., Hatanaka, Y. & Look, D. C. ZnO diode fabricated by excimer-laser doping. *Appl. Phys. Lett.* **76,** 3257–3259 (2000).
12. Ryu, Y. R., Lee, T. S., Leem, J. H. & White, H. W. Fabrication of homostructural ZnO p-n junctions and ohmic contacts to arsenic-doped p-type ZnO. *Appl. Phys. Lett.* **83,** 4032–4034 (2003).
13. Alivov, Y. I. *et al.* Fabrication and characterization of n-ZnO/p-AlGaN heterojunction light-emitting diodes on 6H-SiC substrates. *Appl. Phys. Lett.* **83,** 4719–4721 (2003).
14. Look, D. C. & Claflin, B. P-type doping and devices based on ZnO. *Phys. Status Solidi B* **241,** 624–630 (2004).
15. Haase, M. A., Qiu, J., DePuydt, J. M. & Cheng, H. Blue-green laser diodes. *Appl. Phys. Lett.* **59,** 1272–1274 (1991).
16. Sze, S. M. *Semiconductor Devices: Physics and Technology* Ch. 12 (Wiley, New York, 1986).
17. Chia, C. H. *et al.* Confinement-enhanced biexciton binding energy in ZnO/ZnMgO multiple quantum wells. *Appl. Phys. Lett.* **82,** 1848–1850 (2003).
18. Ohtomo, A *et al.* $Mg_xZn_{1-x}O$ as a II–VI widegap semiconductor alloy. *Appl. Phys. Lett.* **72,** 2466–2468 (1998).
19. Makino, T. *et al.* Band gap engineering based on $Mg_xZn_{1-x}O$ and $Cd_yZn_{1-y}O$ ternary alloy films. *Appl. Phys. Lett.* **78,** 1237–1239 (2001).
20. Takagi, T., Tanaka, H., Fujita, S. & Fujita, S. Molecular beam epitaxy of high magnesium content single-phase wurtzite $Mg_xZn_{1-x}O$ alloy ($x \sim 0.5$) and their application to solar-blind region photodetectors. *Jpn J. Appl. Phys.* **42**, L401–L403 (2003).
21. van de Walle, C. G. Hydrogen as a cause of doping in zinc oxide. *Phys. Rev. Lett.* **85,** 1012–1015 (2000).
22. Theys, B. *et al.* Effects of intentionally introduced hydrogen on the electrical properties of ZnO layers grown by metalorganic chemical vapor deposition. *J. Appl. Phys.* **91,** 3922–3924 (2002).
23. Tsukazaki, A. *et al.* Layer-by-layer growth of high-optical-quality ZnO film on atomically smooth and lattice relaxed ZnO buffer layer. *Appl. Phys. Lett.* **83,** 2784–2786 (2003).
24. Ohtomo, A *et al.* Single crystalline ZnO films grown on lattice-matched $ScAlMgO_4$(0001) substrates. *Appl. Phys. Lett.* **75,** 2635–2637 (1999).
25. Koida, T. *et al.* Correlation between the photoluminescence lifetime and defect density in bulk and epitaxial ZnO. *Appl. Phys. Lett.* **82,** 532–534 (2003).
26. Chichibu, S. F. *et al.* Emission mechanisms of bulk GaN and InGaN quantum wells prepared by lateral epitaxial overgrowth. *Appl. Phys. Lett.* **74,** 1460–1462 (1999).
27. Look, D. C., Hemsky, J. W. & Sizelove, J. R. Residual native shallow donor in ZnO. *Phys. Rev. Lett.* **82,** 2552–2555 (1999).
28. Sumiya, M. *et al.* Quantitative control and detection of heterovalent impurities in ZnO thin films grown by pulsed laser deposition. *J. Appl. Phys.* **93,** 2562–2569 (2003).
29. Ip, K. *et al.* Hydrogen incorporation, diffusivity, and evolution in bulk ZnO. Solid-State Electron. **47,** 2255–2259 (2003).
30. Guo, X.-L., Choi, J.-H., Tabata, H. & Kawai, T. Fabrication and optoelectronic properties of a transparent ZnO homostructural light-emitting diode. *Jpn J. Appl. Phys.* **40**, L177-L180 (2001).
31. Tsukazaki, A. *et al.* Systematic examination of carrier polarity in composition spread ZnO thin films codoped with Ga and N. *Appl. Phys. Lett.* **81,** 235–237 (2002).
32. Ohnishi, T *et al.* Determination of surface polarity of c-axis oriented ZnO films by coaxial impact-collision ion scattering spectroscopy. *Appl. Phys. Lett.* **72,** 824–826 (1998).

Acknowledgements

We thank T. Ohnishi and M. Lippmaa for measurement of coaxial impact-collision ion scattering spectroscopy. This work was supported by MEXT Grant of Creative Scientific Research 14GS0204, MEXT Grant-in-Aid for Young Scientists 15685011, the Asahi Glass Foundation, and the inter-university cooperative program of the IMR. A.T. is supported by a JSPS fellowship and S.F.C. is supported by the MEXT-COE21 program.
Correspondence and requests for materials should be addressed to M.K.

Competing financial interests

The authors declare that they have no competing financial interests.

©2005 Nature Publishing Group